

Supplemental information

Figure legend:

Figure S1. Related to Figure 1

Decreased inflammatory cytokines were observed in the tissues of GdX^{-Y} mice.

(A) The heat map of the downregulated NF-κB target genes (list of 26 genes, absolute log₂ >1, false discovery rate <0.05, p<0.05) in splenocytes of GdX^{-Y} mice and wildtype littermates (n=4) injected with LPS. The mice were injected with LPS (20 mg/kg body weight, ip), and 1.5 hrs after injection, RNA was extracted from their splenocytes and performed the RNA-seq analysis.

(B) GO term analysis of GdX function in the splenocytes of LPS-administrated mice showed one of the most significantly enriched biological process is related to inflammatory response.

(C-E) Deletion of GdX down regulated the gene expression of pro-inflammatory cytokines in the spleen. Quantitative RT-PCR analyses were performed for the mRNA levels of IL-6 (C), TNF-α (D) and IL-1β (E) in the spleen from mice (n=3) treated with LPS.

(F-H) mRNA levels of inflammatory cytokines and GdX in splenocytes (F), thymocytes (G) and hepatocytes (H) were analyzed by RT-PCR from GdX^{+Y} and GdX^{-Y} mice challenged with LPS (20 mg/kg) for 16 h.

(I) The development of different immune cells was normal in GdX^{-Y} mice. The lymphoid tissues were harvested from GdX^{+Y} (n=6) and GdX^{-Y} mice (n=6), and then analyzed the cell numbers of different immune cells and their progenitors. The progenitors were Lin⁻c-kit^{hi}Sca-1⁺ HSC (hematopoietic stem cell), Lin⁻c-kit^{lo}Sca-1⁺CD127⁺ CLP (common lymphoid progenitor), Lin⁻c-kit^{hi}Sca-1⁻CD16/32^{lo}CD34⁺ CMP (common myeloid progenitor), Lin⁻c-kit^{hi}Sca-1⁻CD16/32^{hi}CD34⁺ GMP (granulocyte-macrophage progenitor) and Lin⁻c-kit^{lo}CD135⁺CD115⁺CD11c⁻ CDP (common dendritic cell progenitor).

(J) Protein levels of GdX in different immune cell lines.

(K-M) Different subtypes of FLDCs from GdX^{+Y} and GdX^{-Y} mice were used to measure the production of IL-12 in response to indicated TLR ligand stimulations.

(N) IFN- λ production was decreased in GdX-deficient pDCs after stimulation by TLR agonists for 16 h.

(O and P) Chemokines from GdX-deficient CD24⁻ cDCs were analyzed by ELISA after stimulation by TLR agonists for 16 h. The results were presented as mean \pm SEM from three repeats. *, p < 0.05; **, p < 0.01; ***, p < 0.001.

(Q-T) Cytokine production (IL-6 and TNF- α) in supernatants of GMDCs and BMDMs after LPS stimulation (100 ng/mL) for 16 h were measured by ELISA. The results were presented as mean \pm SEM from three repeats. *, p < 0.05; **, p < 0.01; ***, p < 0.001.

(U) GdX deletion did not influence the apoptosis in DCs after stimulation by TLR agonists. pDCs, CD24⁺ cDCs, CD24⁻ cDCs were incubated with different TLR agonists for 16 h, and apoptosis was detected by FACS with 7-Amino-actinomycin D (7-AAD) and Annexin-V staining. Annexin-V⁺/7-AAD⁻ (early apoptosis) and Annexin-V⁺/7-AAD⁺ (late apoptosis) cells were quantified.

Figure S2. Related to Figure 2

(A) Cell viability assay of HEK293T cells added with various concentrations of lipofectamine 2000. Absorbance was measured at 595 nm with a reference wavelength of 650 nm.

(B and C) GdX promoted the transcriptional activity of NF- κ B. HEK293T cells, with or without over-expression of GdX, were co-transfected with NF- κ B luciferase reporter (NF- κ B-luc) and Renilla luciferase reporter. Relative luciferase activities were determined in three independent experiments after the cells were treated with TNF- α (10 ng/mL) (B) and LPS (100ng/ml) (C) for 8 h.

(D) GdX inhibited STAT3 transcriptional activity. Luciferase activities were determined in HEK293T cells, transfected with the APRE-luc reporter treated with or without LIF.

(E) Depletion of GdX decreased the activity of NF- κ B. Relative luciferase activities were determined with or without depletion of GdX (siGdX, sequences targeting human GdX) after TNF- α (10 ng/mL) treatment.

(F-I) Depletion of GdX decreased the activity of NF- κ B. HEK293T cells were transfected with NF- κ B-luc, together with MyD88 (F), TRAF6 (G), IKK β (H), or p65 (I), along with or without GdXi. Luciferase activity was measured at 36 h after transfection and the results were presented as mean \pm SD from three repeats. **, $p < 0.01$; ***, $p < 0.001$.

Figure S3. Related to Figure 3

(A) GdX failed to interact with p65. HEK293T cells were transfected with the indicated plasmids and IP was performed with a mixture of an antibody against Flag and an antibody against HA.

(B) HA-TC45 interacted with Flag-p65. An IP experiment was performed by using an anti-HA antibody.

(C) TC45 interacted with either p65 or GdX. IP experiments were performed by using anti-Flag, anti-HA or anti-Myc antibody after HEK-293T cells were transfected with Flag-p65, HA-TC45 and Myc-GdX for 24 h. IgG was used as a negative control. This experiment indicated that two separate complexes Flag-p65/HA-TC45 and Myc-GdX/HA-TC45 formed.

(D and E) The interaction of TC45 and p65 was increased in GdX-depleted (KO) GMDCs and BMDMs. GMDCs (D) and BMDMs (E) were used to perform the endogenous IP assay with TNF- α (10 ng/mL) treatment for 15 min. GMDCs and BMDMs from wildtype (WT) mice were used as controls.

(F) A docking model of the competition of GdX with TC45 to interact with p65. While TC45 interacts with p65 (a), there are two helices in TC45 which are free from

interacting with p65 but are able to associate with GdX (b). In this way, GdX occupies the interface of TC45 to complete off p65 (c).

Figure S4. Related to Figure 4

(A) The level of p-p65 was decreased in GdX-depleted splenocytes. Splenocytes were treated with LPS (100ng/ml) and then subjected to starvation for indicated times. Levels of p-p65 imaged at different exposure times (S, short; L, long) were showed.

(B) Over-expression of GdX inhibited p65 dephosphorylation in response to TNF- α treatment.

(C) GdX increased the DNA binding ability of p65. DC2.4 cells were infected by an adenovirus expressing GFP or GdX and were stimulated with TNF- α (10 ng/mL) for the 15 min, and then subjected to starvation. Chromatin was immunoprecipitated with an antibody against p65. PCR was performed by using primers targeting NF- κ B binding sites on the *IL-6* gene promoter. Five percent of the precipitated chromatin was assayed to verify an equal loading (Input).

(D) Real time PCR was used to quantify the amounts of chromatin-immunoprecipitated DNA from B.

Figure S5. Related to Figure 5

(A) A schematic diagram showing domain structures of p65 and its deletions. RHD: rel homology domain. Letter “f” indicated full length protein and different deletions were showed as n1 to n6. Numbers indicated the amino acid positions.

(B) TC45 failed to interact with p65-n6. HEK293T cells were co-transfected with HA-TC45 and Flag-p65 or its deletions as indicated. Flag-tagged proteins were immunoprecipitated with an antibody against HA, and then the complex was blotted with an antibody against Flag.

(C and D) A molecular docking analysis showed Y100 is critical for the interaction of

p65 with TC45. (C) The interface of p65 and TC45 is maintained by F183 and K118 in TC45 and Y100 and P177 in p65. Two reviews are showed on the right panel. (D) A critical band between Y100 at p65 and K118 at TC45 is showed.

Figure S6. Related to Figure 6

(A) The interaction of p65 and PP2A was decreased when TC45 was knock down. TC45 was depleted by transfection with a siRNA targeting TC45 (siTC45) in HEK293T cells for 36 h before harvesting the cells. An IP was performed using an antibody against HA.

(B) p65, PP2A and TC45 formed a complex. IP experiments were performed by using anti-p65, anti-PP2A or anti-TC45 antibody after HEK293T cells were transfected with Flag-p65, HA-PP2A and HA-TC45 for 24 h.

(C and D) The interaction of PP2A and p65 was increased in GdX-depleted cells. GMDCs (C) and BMDMs (D) derived from GdX^{+Y} and GdX^{-Y} mice were used for IP experiments.

(E) GdX(L29P) mutant failed to decrease the interaction of PP2A and p65. HEK293T cells were transfected with the indicated plasmids before the IP experiment.

(F) GdX(L29P) mutant failed to decrease the interaction of PP2A and TC45.

(G) PP2A and TC45 synergistically inhibited the transcriptional activity of NF-κB.

(H) GdX rescued the PP2A-mediated dephosphorylation of p-p65. HEK293T cells were transfected with the indicated plasmids. The protein expression levels were examined by Western blot.

(I) GdX rescued the TC45-induced the inhibition of transcriptional activity of NF-κB.

(J) GdX rescued the PP2A-induced the inhibition of transcriptional activity of NF-κB. Luciferase activity was measured at 36 h after transfection with the indicated plasmids and the results were presented as mean ± SD from three repeats. **, p < 0.01; ***, p < 0.001.

Figure S7. Related to Figure 7

(A-D) The length of colon was determined after DSS treatment. The length of GdX^{-Y} (A), GdX^{ADC} (B), GdX^{ΔMφ} (C) and GdX^{ΔIEC} (D) mice were compared with their WT (Cre-negative) littermates. Results were presented as means ± SD. The numbers of mice in each group is labeled. **P < 0.005.

(E) Intestinal immune cell populations in GdX^{ADC} mice were similar to WT mice during DSS colitis. GdX^{ADC} mice and WT littermate were treated by 3% DSS for 6 day, and then the intestinal immune cells were purified. Splenic and intestinal T_{reg}, intestinal Th17, intestinal F4/80⁻CD11c^{hi} DCs (including CD103⁺CD11b⁻, CD103⁺CD11b⁺ and CD103⁻CD11b⁺ DCs) and F4/80⁺CD11c^{int} Mφs were analyzed by FACS.

Supplemental Experimental Procedures

Isolation of cells from tissues

For isolation DCs from spleen and thymus, tissue was minced with scissors and digested with 0.1 mg/ml DNaseI (Roche Molecular Biochemicals) and 1 mg/ml collagenase III (Worthington Biochemical) at 37°C for 25 min. Then, light-density cells were isolated in 1.077 g/cm³ (spleen) or 1.076 g/cm³ (thymus) Nycodenz (Axis-Shield) medium by centrifugation for 10 min at 1700 g. Additionally, splenocytes were incubated with mAb against CD3, CD90, TER119, Ly6G and CD19, followed by removal of non DC using anti-immunoglobulin (Ig)-coated magnetic beads (Bangs Laboratories). The enriched cells were stained with DC-specific markers and sorted.

For isolation lymphocytes from intestine lamina propria, the small intestine was taken out and removed off the mesentery, Peyer's patches, fat and content. The small intestine was then moved into the medium (RPMI 1640, 1% P/S, 5 mM EDTA, 20 mM HEPES) and shook in 37°C incubator at 190 rpm for 30 min to wash off the epithelial cells. The remaining tissue was minced and digested with 10 U/ml collagenase CLISPA (Worthington Biochemical) and 0.1 mg/ml DNaseI at 37°C for 40 min. Subsequently,

heavy-density cells were purified in 40% Percoll (GE Healthcare) by centrifugation for 10 min at 800 g.

For isolation of BM progenitors, the BM cells were depleted of red blood cells and followed by light-density separation (1.086 g/cm³ Nycodenz, 1700 g, 10 min) and then immune-magnetic bead negative selection (BM lineage cocktail: CD2, CD3, CD8, B220, CD11b, TER119, Ly6G).

Other immune cells were isolated from spleen, thymus and BM after removal of red blood cells.

Flow cytometry and antibodies

Single-cell suspensions were prepared and blocked in rat immunoglobulin (Jackson Laboratories) for 10 min for flow cytometry analyses. For cell surface markers, antibody incubation was performed at 4°C for 30 min. For intracellular Foxp3 staining, the Foxp3 Staining Buffer Set (eBioscience) was used. For intracellular IL-17A and TLR9 staining, we used Fixation /Permeabilization solution kit (BD). The following mAbs were used for cell staining and sorting: PE-Cy7-conjugated CD11c (N418), CD45R (RA3-6B2) and Ly6A/E (D7), PE-conjugated Siglec-H (eBio440c), F4/80 (BM8), CD3e (eBio500A2), CD135 (A2F10), Foxp3 (NRRF-30), IL-17A (eBio17B7), TLR2 (6C2) and CD103 (2E7), FITC-conjugated CD172 α (P84), Ly6G (1A8), CD4 (GK1.5), CD16/32 (2.4G2), CD11c (N418), CD45R (RA3-6B2) and TLR9 (M9.D6), APC-conjugated CD8 α (53-6.7) , CD11b (M1/70), CD19 (eBio103), CD117 (ACK2), CD25 (PC-61.5.3), F4/80 (BM8) and CD24 (M1/69), eFluor 450-conjugated CD8 α (53-6.7) and MHC- II (M5/114.15.2), APC-cy7-conjugated CD45 (30-F11), BV605-conjugated CD11b (M1/70), biotinylated CD127 (A7R34), CD34 (RAM34) and CD115 (AFS98). PE-streptavidin and PE-Cy7-streptavidin were used for second-stage staining. All of the antibodies were purchased from eBioscience, BD Biosciences or BioLegend. Dead cells were discriminated in all experiments using 7-AAD (eBio) staining. Cell apoptosis was analyzed by AnnexinV apoptosis detection kit (eBio). Cell analysis was carried out on LSRII and LSRFortessa

flow cytometers; cell sorting was performed on FACS Aria II and FACS Aria III instruments. All of the machines were purchased from BD Bioscience. The purity of sorted populations was routinely more than 95%. Data analysis was performed on the single, live cell gate using FlowJo software (TreeStar).

Antigen presentation assay

The OT-I CD8⁺ and OT-II CD4⁺ T cells were isolated from the spleen of OT-I or OT-II transgenic mice, through depletion of red blood cells and immune-magnetic bead negative selection (CD8⁺ T cell cocktail: CD11b, F4/80, B220, CD11b, CD19, TER119, Ly6G, MHC-II, CD4; CD4⁺ T cell cocktail: CD11b, F4/80, B220, CD11b, CD19, TER119, Ly6G, MHC-II, CD8). And then the T cells were labeled using CFSE cell proliferation kit (Invitrogen).

Splenic CD8⁺ cDCs and CD8⁻ cDCs (1×10^5 cells/ml) were sorted and incubated in 24-well plates (Costar-Corning) with OVA protein (100 ug/ml, Sigma) or OVA peptide (CD8⁺ cDCs: OVA₂₅₇₋₂₆₄, 1 ng/ml; CD8⁻ cDCs: OVA peptide₃₂₃₋₃₃₉, 10 ug/ml, Sigma) at 37 °C in RPMI 1640 complete medium. After 2 h, cells were washed twice. DC populations were plated with different numbers in 96-well round-bottom plates. Ten thousand CFSE-labeled OT-I or OT-II T cells (OT-I CD8⁺ T cells: CD8⁺ cDCs; OT-II CD4⁺ T cells: CD8⁻ cDCs) were added in each well in RPMI-1640 complete medium supplemented with 20 ng/ml GM-CSF. Proliferation was analyzed by flow cytometry after 60–90 h of culture.

Chromatin Immunoprecipitation (ChIP) Assay

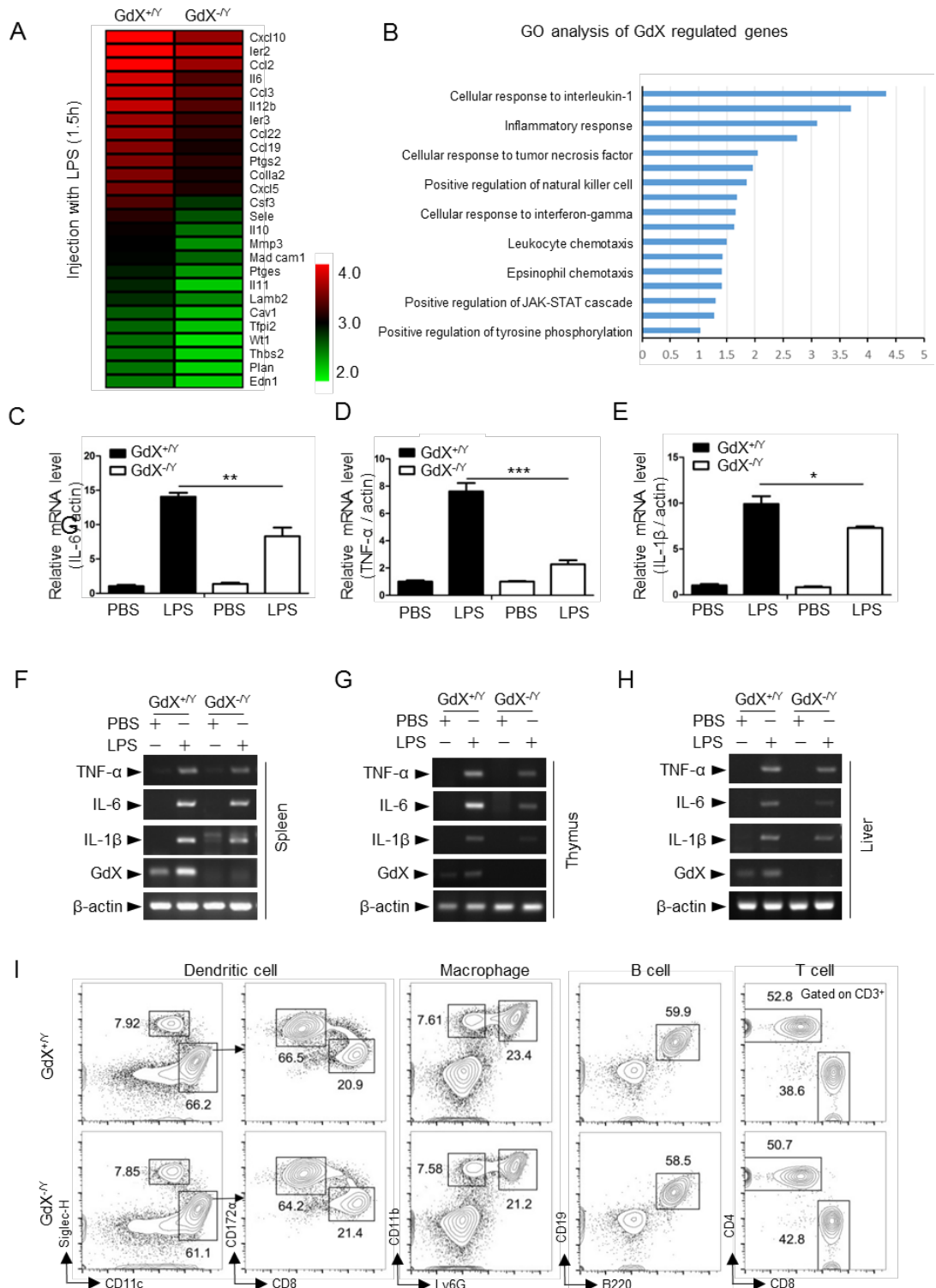
A modified protocol from Upstate Biotechnology was used. Briefly, cells were fixed at 37°C for 10 min with 1% formaldehyde for crosslinking. The cells were resuspended in 500 ul of ChIP lysis buffer and mixed at 4°C and then sonicated for 30 s at level 2 (Ultrasonic Processor, Sonics) to yield DNA fragments that were 100–500 bp in size. Eluted DNA was recovered with QIAquick columns (Qiagen, Germany) and used as templates for PCR amplifications. The input control was from the supernatant before

precipitation. The fragment corresponding to the NF- κ B binding site in the IL-6 promoter was amplified by PCR with primers 5'-TGCTCAAGTGCTGAGTCACT-3' and 5'-AGACTCATGGGAAAATCCCA-3'. Real time PCR was used to quantify the precipitated DNA fragments.

Immunofluorescent Analysis

Hela cells were plated on glass coverslips in 6-well dishes, incubated overnight at 37°C, and then infected with adenovirus. 24 h after infection, cells were rinsed with PBS three times, fixed with 4% paraformaldehyde in PBS for 15–20 min at room temperature, and permeabilized with 0.2% Triton X-100 in PBS for 10 min. Cells were blocked with 10% goat serum for 1 h at room temperature. The primary antibodies, diluted in PBS with 3% bovine serum albumin, were incubated overnight at 4°C, and bound antibodies were detected with secondary antibodies conjugated with TRITC (red) for 1 h at room temperature. Finally, cells were stained with DAPI. Stained cells were analyzed with a laser scanning confocal microscopy (OLYMPUS FV10i-Oil).

Figure S1 related to Fig. 1



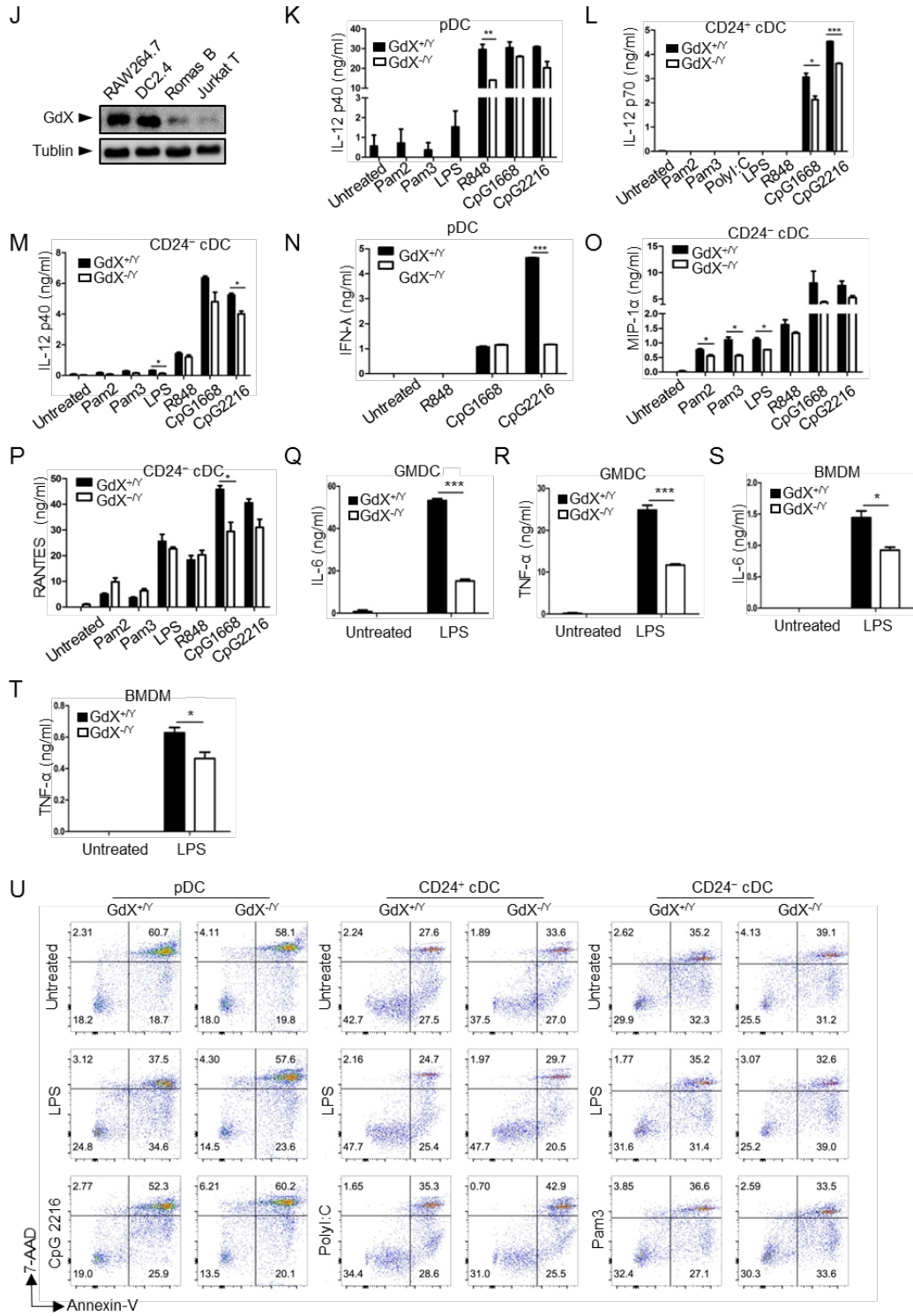


Figure S2 related to Fig. 2.

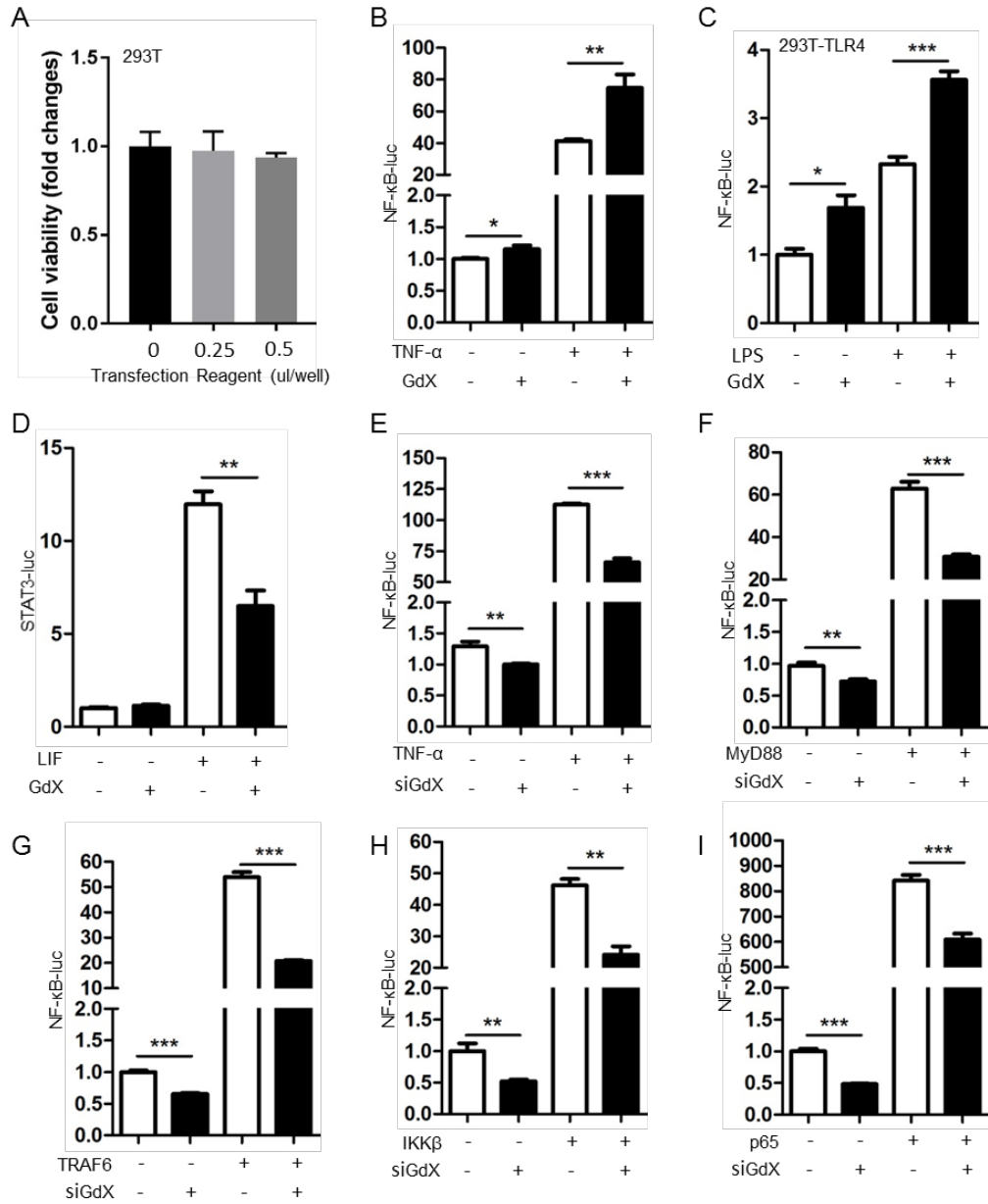


Figure S3 related to Fig. 3

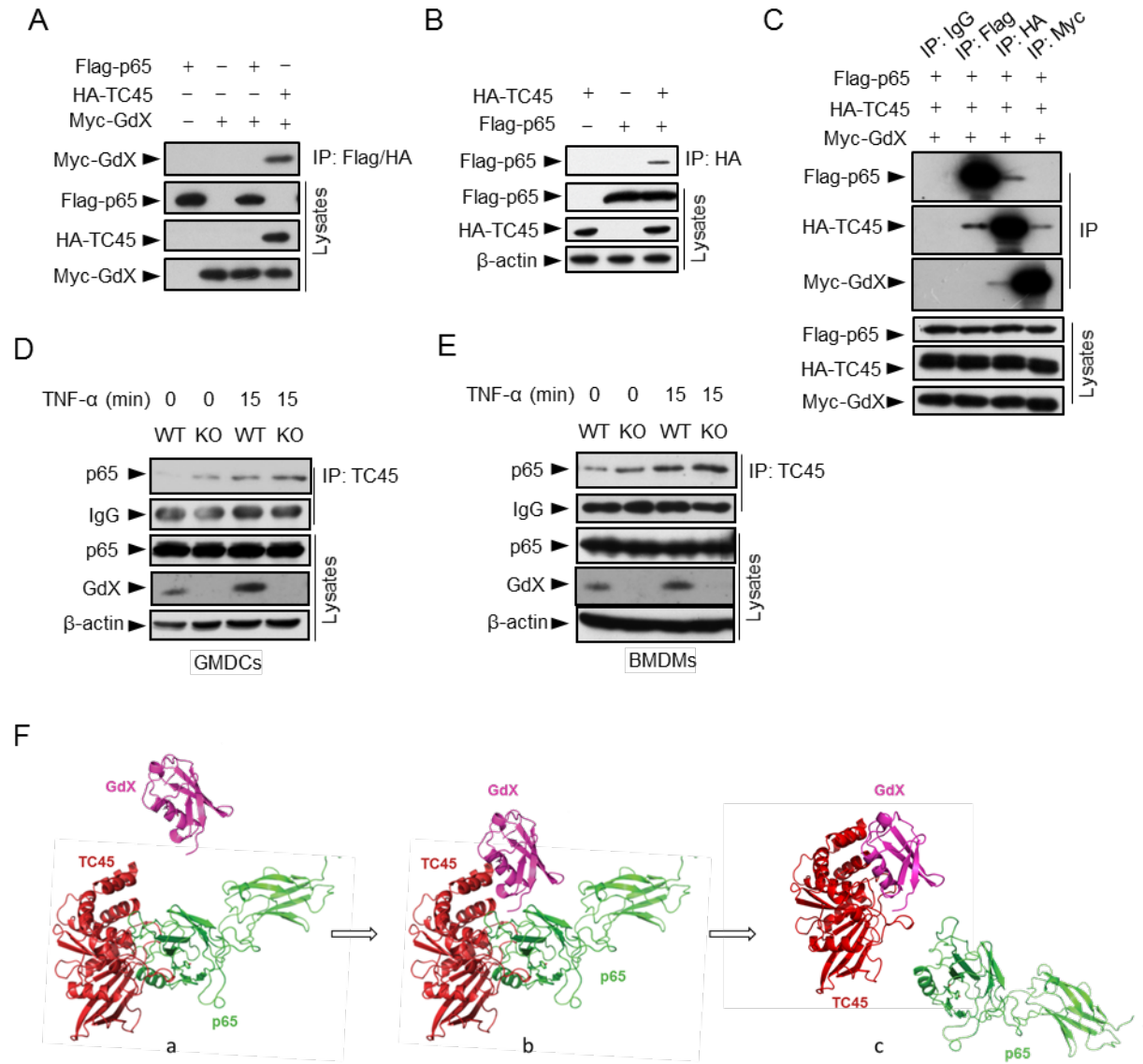


Figure S4 related to Fig. 4.

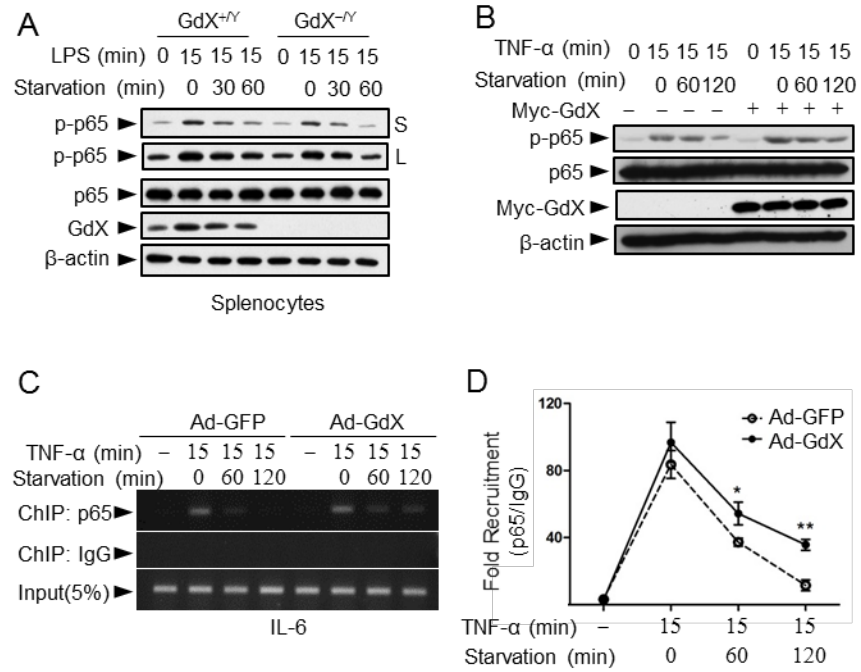


Figure S5 related to Fig. 5.

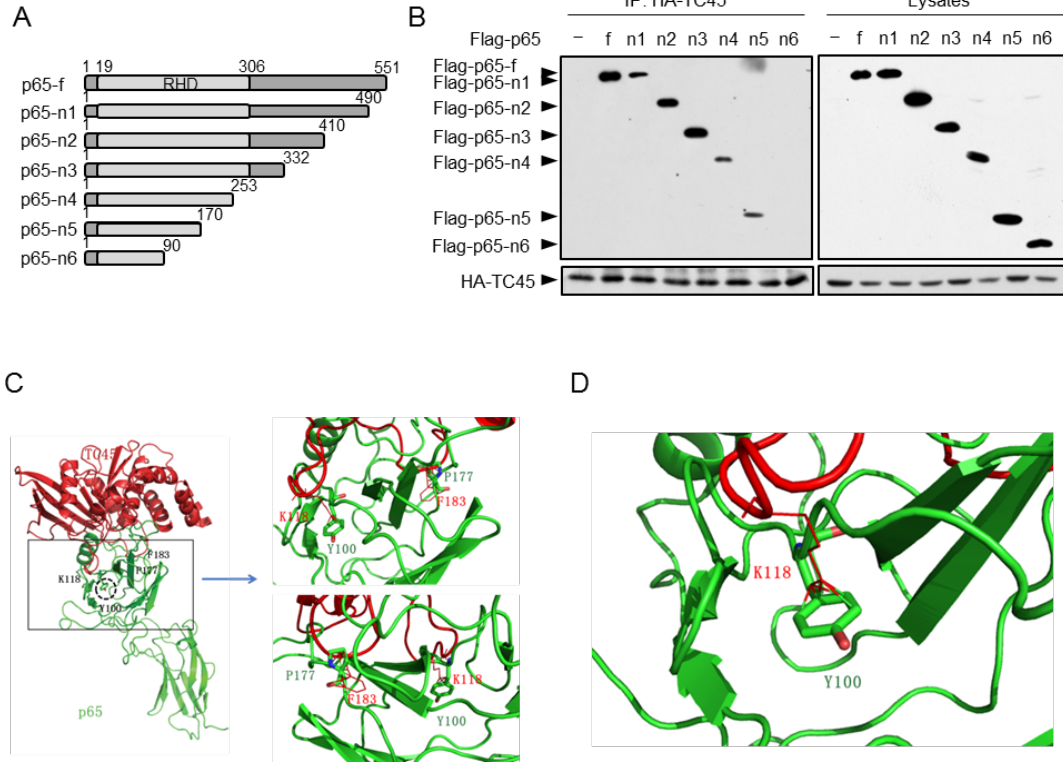


Figure S6 related to Fig. 6.

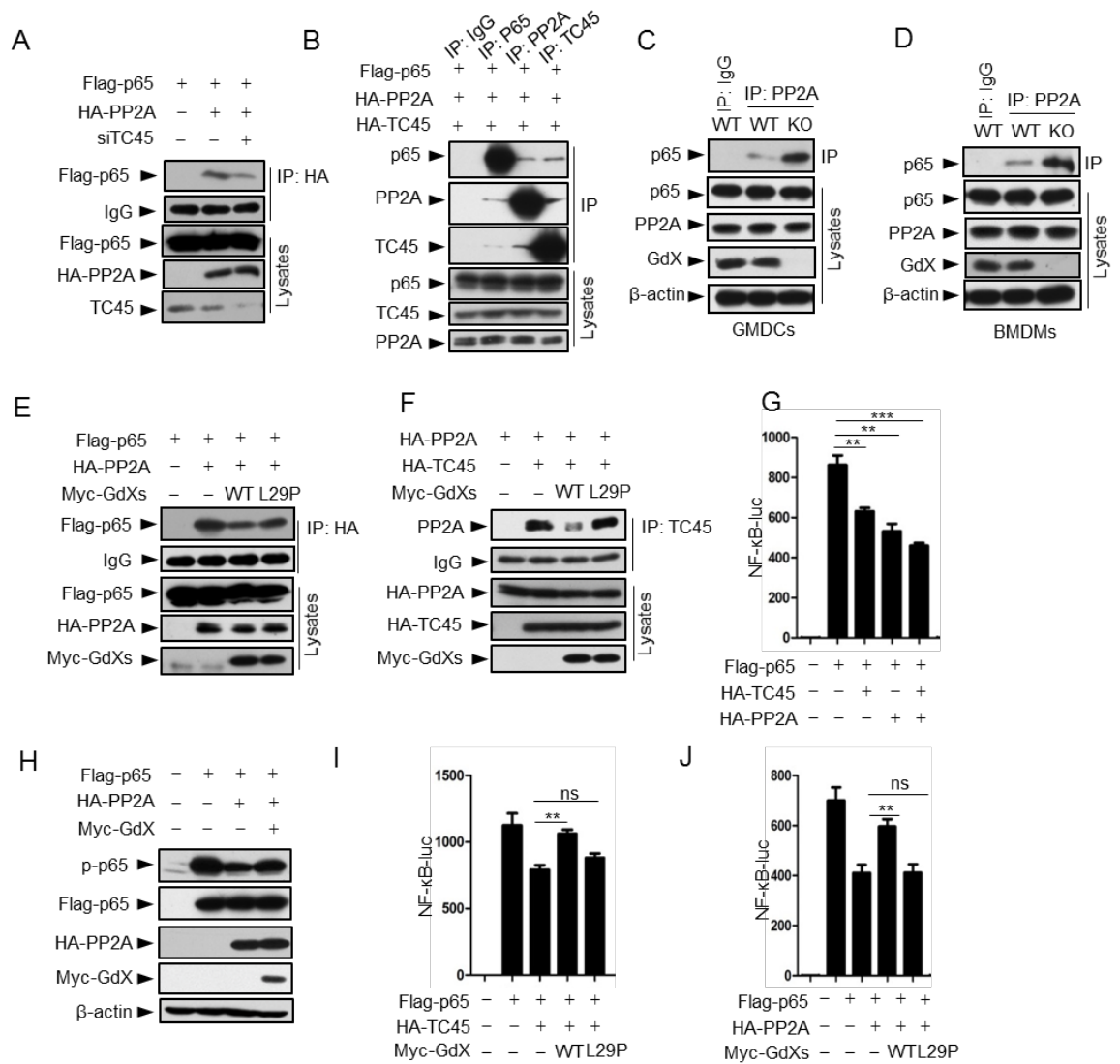


Figure S7 related to Fig. 7.

